

Reproducible Peak Clusters on Differential Mouse Mortality Curves and Their Relation to the Gompertz Model

A. G. Malygin^{1,a}

¹Bach Institute of Biochemistry, Research Center of Biotechnology, Russian Academy of Sciences, 119071 Moscow, Russia
^ae-mail: agmalygin@mail.ru

Received October 27, 2017
Revision received March 28, 2018

Abstract—It is shown that differentiation of mouse mortality curves (number of animals that died at a certain age plotted versus their lifespan) results in the appearance of eight clearly distinguished clusters of peaks corresponding to increased mortality rates. Smoothing of the original mortality curves and subsequent transformation of the differential mortality curves according to the Gompertz model makes the peaks and the corresponding clusters less pronounced and drives the logarithm of the force mortality curve toward a straight line. The positions of the clusters on the lifespan axis (expressed in days) were calculated as weighted means by dividing the sum of the products of multiplication of the peak heights and their position on the lifespan axis by the sum of the peak heights within a cluster. To prove that the peaks and their clusters are not random, we have demonstrated that the positions of the clusters on the lifespan axis do not depend on the extent of mortality curve smoothing or the group of mice analyzed.

DOI: 10.1134/S0006297918070076

Keywords: lifespan, mice, differential mortality curves, peak clusters, Gompertz model

Data on the lifespan of large human populations are usually presented as mortality (or survivorship) curves, which show the dependence of the number (or proportion) of individuals that have died by a certain age (or survived to this age, respectively) on their lifespan. These curves are often smoothed by averaging the data for tens or even hundreds of thousands of individuals and transforming them into the force of mortality curves by the formula published by Gompertz, an insurance company employee, in 1825 [1]:

$$\mu(x) = dl_m(x)/[l(x)dx], \quad (1)$$

where $\mu(x)$ is force of mortality function; x is lifespan (age); $l_m(x)$ is mortality function (number of individuals that have died by this age); $l(x)$ is survivorship function (number of individuals that have survived by this age); and $dl_m(x)/dx$ is a derivative that reflects the mortality rate for individuals of a given age. The mortality and survivorship functions complement each other and are related by the equation:

$$l(x) = l_0 - l_m(x), \quad (2)$$

where l_0 is the initial number of individuals in the studied population.

Gompertz showed that force of mortality curves plotted using statistical data for individuals 35-90 years of age can be adequately described by an exponential dependence that includes only two parameters:

$$dl_m(x)/[l(x)dx] \approx R \exp(\alpha x), \quad (3)$$

where R and α are values typical of a studied population. The logarithm of the exponent is a straight line:

$$\ln \mu(x) \approx \ln[R \exp(\alpha x)] = \ln R + \alpha x. \quad (4)$$

In the past, when computer technology was not available, the two-parameter Gompertz model considerably facilitated the processing of statistical data. The deviation of the logarithm of the experimental force of mortality curve from a straight line for individuals of ages 1 to 35 and over 90 [2, 3] did not concern insurance companies and demographers because the portion of people dying within these age intervals did not exceed 2% of the total studied population.

However, when the Gompertz formula was used for describing mortality of genetically identical animals, whose populations in laboratories are orders of magnitude smaller than the studied human populations, the loga-

rithm of the force of mortality curve failed to represent a straight line [4]. This discrepancy has been mostly explained by random variations in the lifespan, thereby suggesting that with increase in the number of experimental animals, the logarithm of the force of mortality curve could be approximated by a straight line (as it occurs for human populations).

But what are random variations? We often call some phenomenon random because we simply do not know the underlying reason. According to a well-known definition, an accidental event is an unrecognized regularity. In turn, regularity is a stable reproducible connection between processes and their manifestations. Therefore, deviations from theoretical curves describing some natural phenomena remain random only until their connection with some other processes is revealed. The Gompertz formula is a law to an extent to which it reflects in the first approximation the relationship between mortality and lifespan. However, if deviations from the Gompertz law happen consistently during certain lifetime periods in independent groups of animals, they cease to be random and become new regularities that cannot be described by the Gompertz formula. The existence of reproducible peaks of accelerated mouse mortality on the differential mortality curves was described in my previous publication [5]. Since the regularities in the positions of these peaks on the lifespan axis had not been noticed before, the phenomenon was accepted with considerable skepticism from some researchers, which resulted in a delay in the publication of this phenomenon. Most objections came to the question: why have these peaks not been discovered before? The goal of this study was to elucidate the reasons that prevented earlier discovery of regular deviations on the mortality curves and to confirm again the existence of increased mortality peaks by identification of peak clusters with reproducible positions on the lifespan axis.

Another objective of this study was to eliminate the contradictions between reproducible peaks on the differential mortality curves and the description of mortality by smooth curves of the Gompertz model.

MATERIALS AND METHODS

The mice used in this study were progeny of normal females and mutant males with a growth delay from a heterogeneous laboratory population. The original mutant male described in [5-8] was accidentally discovered in the offspring of a wild-type white female and a male treated with AgNO_3 . The number of normal mice in the progeny considerably exceeded the number of mutants. Since the peak positions of mortality rate on the differential mortality curves for the mutant mice differed from those observed for the normal mice, the mutant mice were excluded from this study. To increase the studied cohort, the lifespan data from this study were combined with the

data from [5], so that the total number of normal mice was 558 (256 males and 302 females). The birth and death dates of the mice have been recorded for nine years. For characteristics of the studied mouse population, breeding strategies, housing conditions, and data processing methods, see publications [5-8].

To prove the independence of the positions of peak clusters on the lifespan axis on the extent of curve smoothing, the mortality curves were plotted for all mice as a function of the number of specimens that had died by a certain age on their lifespan.

To reveal the reproducibility of the peak positions on the lifespan axis in independent groups of animals, the total mouse population (both males and females) was ranked according to the increase of half-lifespan (time-point between mouse birth and death) (Table S1 in Supplement to this paper on the site of *Biochemistry* (Moscow) <http://protein.bio.msu.ru/biokhimiya> and Springer site [Link.springer.com](http://link.springer.com)) and then divided into two equal subgroups by two different methods. In the first case, the resulting cohort was split in the middle into two subgroups. In the second case, the subgroups were formed from odd and even members of the cohort, respectively.

The use of the half-lifespan allowed to avoid enrichment of the first subgroup and depletion of the second subgroup with the data on the lifespan of long-living mice, when ranking the mice according to the birth date, and *vice versa*, depletion of the first subgroup and enrichment of the second subgroup with the data on the lifespan of long-living mice, when ranking the mice according to the date of death.

Mortality curves have been plotted for each of the subgroups and for the mixed group of males and females and then smoothed as described below and in [5].

Similarly to the procedure used in [5], differential mortality curves were obtained by numerical differentiation of the smoothed mortality curves. Numerical differentiation includes division of the difference between the adjacent values of mortality Δl_m on the y -axis by the distance Δx between these values on the x -axis according to formula (5):

$$dl_m(x)/dx \approx \Delta l_m / \Delta x. \quad (5)$$

The lifespan on the initial mortality curves was expressed in days (integers). If the lifespans of several mice were the same, the distance between the corresponding values on the x -axis equaled zero ($\Delta x = 0$), i.e., the derivative at these points becomes infinity. To avoid this situation, the mortality curves were smoothed before differentiation by calculating the rolling average. The new positions of the data points on the x -axis were calculated by adding the lifespan values for the points within the averaging interval and then dividing the sum by the number of such points. The averaging interval was then moved by one point to the right along the x -axis. This procedure

Table 1. Positions of major peak midlines, cluster borders, and clusters on differential mortality curves at different averaging intervals

Number of major peak and corresponding cluster	Mean position of major peaks on lifespan axis, days	Position of cluster borders on lifespan axis, days	Weighed mean positions of clusters on lifespan axis (x_{cl}), days				
			number of original mortality curve points within the averaging interval				mean arithmetic positions of cluster groups, days
			6	11	21	31	
1	391.9	366.0	397.4	395.1	396.6	396.1	396.3
2	443.2	417.6	447.2	449.2	447.9	449.1	448.4
3	497.2	470.2	492.9	493.7	494.9	494.2	493.9
4	533.3	515.2	532.9	532.0	531.9	530.7	531.9
5	577.6	555.4	580.1	578.9	579.6	579.2	579.4
6	625.6	601.6	629.9	629.9	629.0	628.6	629.3
7	683.6	654.6	685.0	684.1	682.3	682.1	683.4
8	747.0	715.3	740.9	738.2	738.4	737.6	738.8
		778.7					

was repeated until adjacent points on the mortality curve are over. To exclude the appearance of infinite values during mortality curve differentiation, the number of points within the averaging interval should equal to or exceed the number of subjects with the same lifespan on the initial mortality curve. For example, if the maximal number of subjects with the same lifespan is six, the number of points, and respectively, lifespan values in the averaging interval should be six or more.

After smoothing, the number of mice on the l_m axis remained an integer, while the number of days (lifespan) on the x -axis became a fractional number. For this reason, the positions of the differential mortality curve points on the x -axis are given as fractional values with an accuracy of 0.1 day (Tables 1 and 2 and Supplementary Tables S2 and S3).

The peak clusters on the differential mortality curves were identified visually; then their exact positions on the

lifespan axis were found in several steps. First, the positions of the tallest peaks in the clusters were determined. Such peaks were denoted as major peaks, to be distinguished from the smaller minor peaks. Then, the arithmetical means for the positions of the apexes of the corresponding major peaks were determined. These values were used to plot the midlines vertically connecting major peaks on the compared curves. These midlines were then applied to define the cluster borders. The borders between adjacent clusters were calculated as mean values for the positions of the midlines. The outer borders of the outermost left and right clusters on the differential mortality curves were considered to be symmetrical to the right and left borders, respectively, of these clusters with the adjacent ones.

The exact positions of clusters on the lifespan axis (in days) were determined as weighed arithmetical means calculated by dividing the product of multiplication of

Table 2. Positions of major peak midlines, cluster borders, and clusters on differential mortality curves in independent groups of mice

Number of major peak and corresponding cluster	Mean position of major peaks on lifespan axis, days	Position of cluster borders on lifespan axis, days	Weighed mean positions of clusters on lifespan axis (x_{cl}), days				
			mouse subgroups				mean arithmetic positions of cluster groups, days
			1st subgroup (half)	2nd subgroup (half)	odd number subgroup	even number subgroup	
1	397.2	369.3	395.1	399.3	395.9	397.1	396.9
		425.1					
2	453.1	474.9	451.8	453.8	452.8	451.7	452.5
		496.8					
3	496.8	513.6	496.9	496.6	496.7	494.7	496.3
		530.5					
4	530.5	557.0	530.8	530.1	531.2	526.3	529.6
		583.5					
5	583.5	606.7	579.2	576.2	579.4	577.9	578.2
		630.0					
6	630.0	653.4	631.6	629.2	630.9	628.0	629.9
		676.8					
7	676.8	708.2	676.9	678.5	677.4	678.5	677.8
		739.7					
8	739.7	771.1	734.2	733.0	733.3	734.8	733.8

peak positions on the lifespan axis and peak heights by the sum of peak heights within a cluster according to formula (6):

$$x_{cl} = \frac{\sum_{i=1}^n (\Delta I_m / \Delta x)_{\max i} \cdot x_{\max i}}{\sum_{i=1}^n (\Delta I_m / \Delta x)_{\max i}}, \quad (6)$$

where x_{cl} is the cluster position on the lifespan axis, days; i is peak number in the cluster or background region corresponding to the peak in the compared differential mortality curve; n is the number of peaks in the cluster including background regions corresponding to the peaks in the compared differential mortality curves; $(\Delta I_m / \Delta x)_{\max i}$ is peak height or height of the background region corresponding to the peak in the compared differential mortality curve expressed as the number of mice that died per

day; $x_{\max i}$ is peak position or position of the corresponding background region on the lifespan axis, days.

The absence of the corresponding peak on one of the compared differential mortality curves in some cases meant that the height of this peak was similar to the background mortality rate in the studied fragment of the curve. In such cases, the value of the peak height in the formula was replaced by the value of the corresponding background fragment of the curve.

RESULTS AND DISCUSSION

Clusterization of mortality peaks and their hiding because of Gompertz transformation. Transformation of the lifespan data in the Gompertz model includes four stages: 1) smoothing of the original mortality curve; 2) numerical differentiation of the smoothed curve;

3) transformation of the differentiation mortality curve into the force of mortality curve; and 4) linearization of the force of the mortality curve by taking the logarithm. To find the stage at which detailed information on the mortality curve shape is lost, I performed Gompertz transformation using our experimental data. The results are shown in four panels in Fig. 1 (a, b, c, and d) corresponding to the stages of Gompertz transformation. Since the curves were transformed after smoothing by averaging over 6, 11, 21, and 31 points, each panel in Fig. 1 shows four graphs corresponding to different degree of smoothing. The number 6 was the minimal number of values within the averaging interval that was required for eliminating the appearance of infinite values on the differential curves. The other three numbers (11, 21, and 31) were obtained by successive increasing the averaging interval by 10 points, starting from first.

Figure 1a shows smoothed mortality curves that were plotted using rolling averaging over 6, 11, 21, and 31 points (bottom to top; $a(6)$, $a(11)$, $a(21)$, and $a(31)$, respectively). It is clearly seen that, despite slightly decreasing waviness, all mortality curves look alike. The values of points on the curves could be calculated from the lifespan data (Table S2 in Supplement) as described in "Materials and Methods".

Figure 1b shows differential mortality curves obtained by numerical differentiation of the mortality curves smoothed by formula (5). Similarly to Fig. 1a, the curves are designated $b(6)$, $b(11)$, $b(21)$, and $b(31)$ (bottom to top) according to the number of points in the averaging interval. The coordinates of points on the differential mortality curves are shown in Table S2 (see Supplement).

Figure 1c shows the force of mortality curves obtained by division of the values from the differential mortality curves on the corresponding values on the survivorship curves and designated as $c(6)$, $c(11)$, $c(21)$, and $c(31)$. Since the survivorship curves eventually approach zero, the terminal parts of the force of mortality curves raise upward abruptly, while the major parts of these curves remain close to the x -axis. For this reason, the peaks at the terminal parts of the force of mortality curves are much more pronounced. The most distinguishable peaks on the force of mortality curves correspond to the major peaks on the differential mortality curves (designated with vertical lines with the same numbers). As the extent of averaging increases, the peaks become less noticeable, so that it appears that within the averaging interval the curves could be adequately approximated by the exponent $\mu(x) \approx R \exp(\alpha x)$, as according to Gompertz.

Figure 1d shows the last stage of the mortality curve transformation according to Gompertz, namely the logarithms of the force of mortality curves (designated $d(6)$, $d(11)$, $d(21)$, and $d(31)$). According to formula (4), they are approximated by inclined straight lines. Although tak-

ing the logarithm abolishes rapid increase of the exponent, the incline of the resulting line restricts the limits of stretching of individual peaks along the y -axis. Therefore, the amplitude of variations of the logarithms of the force of mortality values is much smaller than in the differential mortality curves (Fig. 1b). The peaks are also hidden with the increase in the extent of averaging. The maximal deviations from the inclined lines in Fig. 1d correspond to the major peaks in Fig. 1, b and c. As in the previous cases, they are connected by numbered midlines.

The values of points on the experimental curves in Fig. 1, c and d, can be calculated from the data presented in Table S2 (see Supplement) using formulas (1)-(4).

Smoothing by averaging the original data is a common approach for the refinement of experimental curves. However, this procedure is no more than a distortion of the experimental curve that results in the loss of the information on its true shape. The latter could be convincingly demonstrated for smoothing of $\sin x$ or $\cos x$ trigonometric functions. At a given point density, these curves are flattened with increase in the number of points within the averaging interval and eventually become straight lines coinciding with the horizontal axis.

The natural reason for a smooth shape of the initial mortality curves is averaging of data due to genetic variability of studied populations resulting in shift of variations in the lifespan of individuals. The effect of this factor was demonstrated in my previous study [5], when genetic differences between normal and mutant mice required the use of different numeration systems for identification of peaks on the differential mortality curves.

Analysis of data presented in Fig. 1 reveals three reasons for the disappearance of peak clusters and their components on the curves obtained by Gompertz transformation.

The first reason is extra (in addition to natural) smoothing of mortality curves that is usually done before Gompertz transformation by calculating mean values for points within equal intervals on the lifespan axis (and not by using rolling averaging described in "Materials and Methods"). The number of mean values in this case corresponds to the number of intervals, and therefore any regularities that are comparable in size with the intervals are easily lost.

The second reason is that division of values from the differential curves by the values from the survivorship curves masks irregularities on the major part of the resulting force of mortality curve.

The third reason is that logarithmic transformation of the force of mortality curve is insufficient to eliminate the effects of the second reason. As a result, deviations from the Gompertz model remained unnoticed.

Based on all the above, differential mortality curves (Fig. 1b) obtained from minimally smoothed mortality curves are more suited for efficient identification of irregularities in the mortality patterns in animal ontogenesis

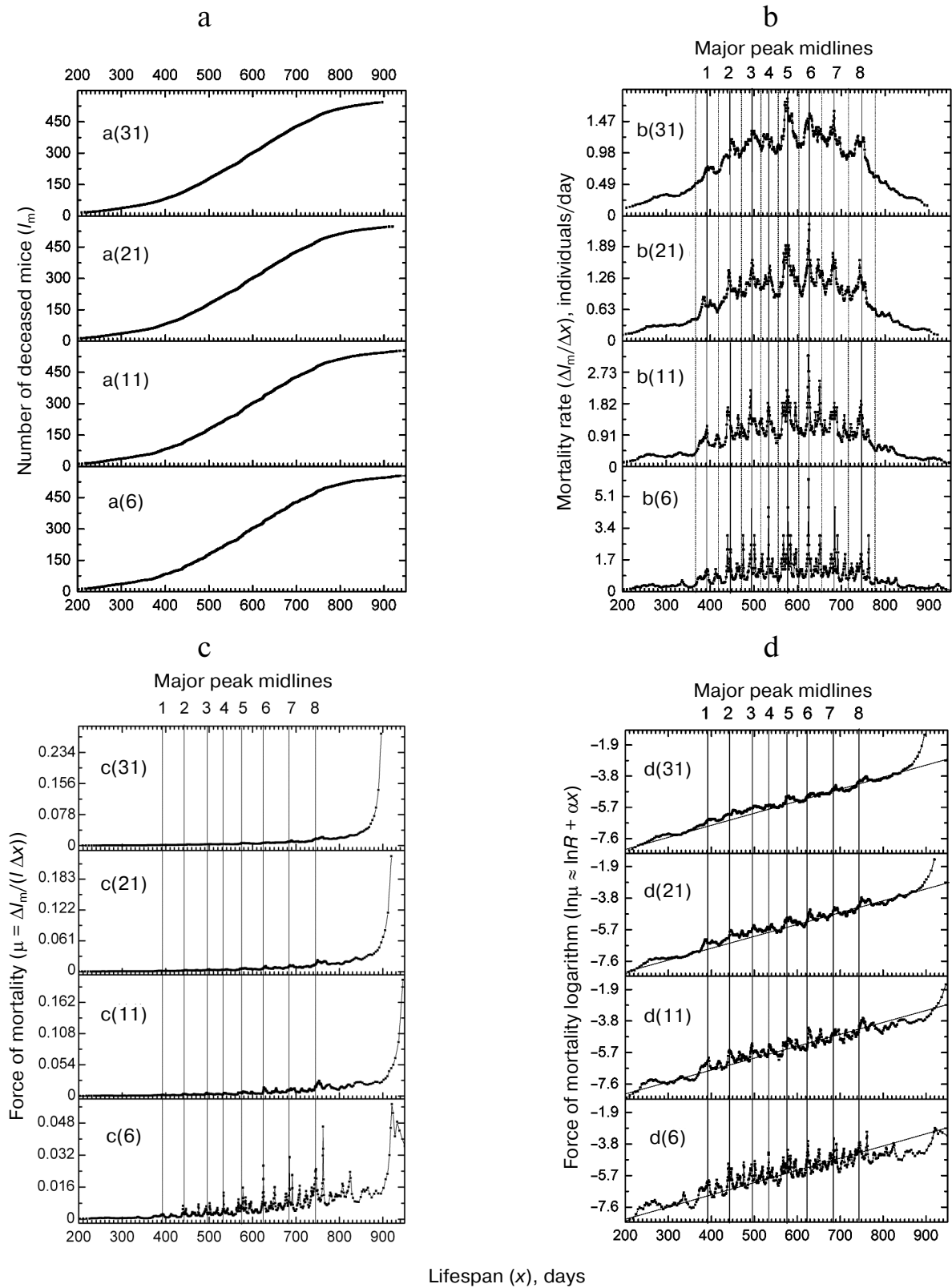


Fig. 1. Curves obtained at different stages of Gompertz transformation of mouse lifespan data for different extents of smoothing of the original mortality curves: a) smoothed mortality curves; b) differential mortality curves; c) force of mortality curves; d) logarithms of force of mortality curves. The number of points within the interval used for rolling averaging of the initial mortality curves is shown in parentheses; solid vertical lines are major peak midlines; dashed lines are cluster borders.

than the force of mortality curves or their logarithms (Fig. 1, c and d). Indeed, barely noticeable inflexions in the mortality curves (Fig. 1a) become very pronounced after differentiation and produce a clearly visible system of clusters composed of major and minor peaks (Fig. 1b). Increasing the number of points within the averaging interval from 6 to 31 results in the decrease in the size and number of peaks in the clusters due to their merging, as well as in well-defined separation of clusters. The clusters are separated from each other by intervals corresponding to ages with decreased mortality rate. In the first approximation, the positions of clusters on the lifespan axis are determined by the positions of major peaks. Thus, in Fig. 1 the major peaks are near continuous midlines that transverse panels (b)-(d). The cluster borders in Fig. 1b are indicated with dashed lines. The positions of the midlines and cluster borders on the lifespan axis are shown in Table 1, as calculated from the data on the positions of major peaks (see Table S2 in Supplement) according to the procedure described in "Materials and Methods". As a result, eight midlines were obtained (Fig. 1, b-d, numbered from top to bottom). The distances between the major peaks vary within 40-50 days, which is significantly longer than peak displacement from the midlines (less than 10 days).

The minor peaks in the plots are less reproducible than the major ones and comprise additional components of the clusters. With very few exceptions, minor peaks are considerably smaller than the major peaks.

Since the clusters include both major and minor peaks, their positions on the lifespan axis could not be

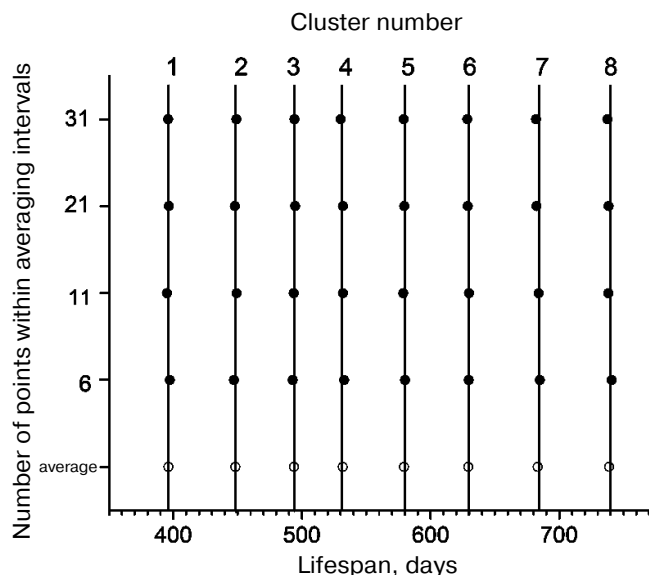


Fig. 2. Weighed positions of eight clusters on the lifespan curves obtained by rolling averaging of the original mortality curves using averaging intervals of 6, 11, 21, and 31 points relative to the mean arithmetic positions of the clusters (designated by vertical lines).

determined with precision based solely on the positions of major peaks. Therefore, weighed arithmetic mean was calculated by formula (6) using positions of all peaks in the cluster. The results of these calculations are shown in Table 1 and Fig. 2. It is evident that positions of the clusters on the lifespan axis are stable and have virtually no dependence on the extent of mortality curve smoothing, which indicates that their presence on the differential mortality curves is not random.

Proof for reproducibility of positions of peak clusters on differential mortality curves. It is possible that the main reason for the fact that no reproducible irregularities on the mortality curves had been conclusively identified before is the absence of comparative studies of mortality curves in independent groups of animals because of the large amount of time required for such type of experiments. However, these studies are essential for proving the existence of real deviations of the experimental mortality curves from the theoretical ones. For this reason, discovering the clusters of peaks of increased mouse mortality and revealing the independence of their positions on the lifespan axis on the extent of curve smoothing should be followed by showing that these clusters and their constituent peaks are reproducible on differential mortality curves. To do this in independent experiments, all mice were divided into subgroups by two methods (see "Materials and Methods"). Separation of the ranked cohort of mice into two halves resulted in two independent subgroups of lifespan data that corresponded to studies performed subsequently at different times. When the mice were divided into subgroups by the second method (into even and odd subjects), the data could be considered as independent results from two randomly selected groups, thereby imitating independent studies performed concurrently. The resulting mortality curves were smoothed using the 15-point averaging interval, which is a half of the maximal investigated averaging interval (31 points).

The results of numerical differentiation of the smoothed mortality curves are shown in Table S3 (see Supplement). Differential mortality curves for four mouse subgroups are shown in Fig. 3. As in the previous case, they exhibit eight clearly distinguishable clusters composed of major and minor peaks. The values for the major peak midlines and cluster boundaries on the lifespan axis (Table 2) were calculated as described in "Materials and Methods" based on the positions of major peaks (see Table S3 in Supplement).

Because the clusters included both major and minor peaks, the positions of the major peaks only were insufficient for determining the positions of clusters on the lifespan axis. The more precise positions of the clusters were calculated as weighed arithmetic means of the peak positions in the clusters by formula (6). The results of calculations (Table 2 and Fig. 4) demonstrate that the positions of the clusters on the lifespan axis are stable and have vir-

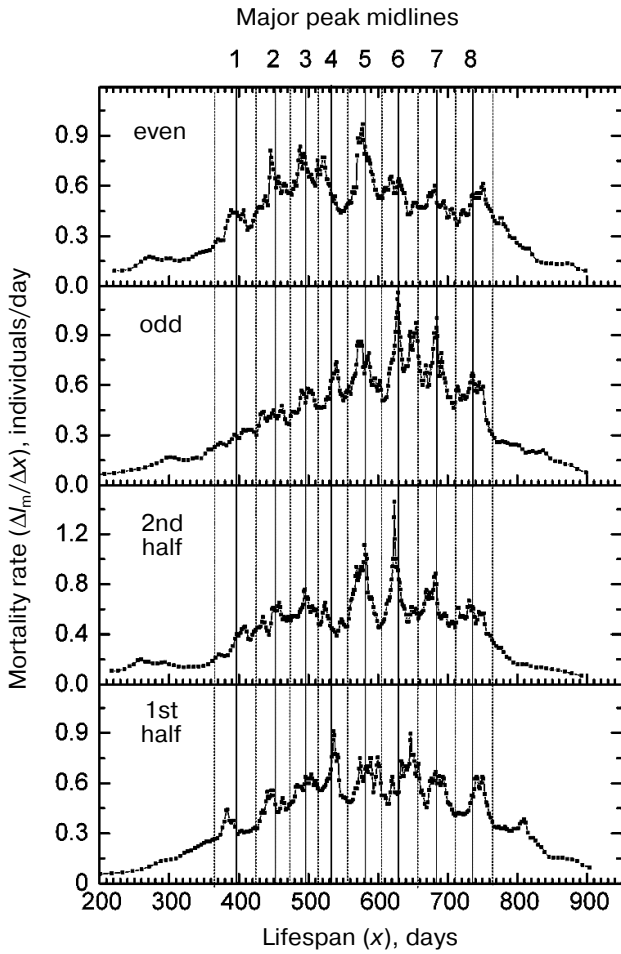


Fig. 3. Differential mortality curves after rolling averaging of initial mortality curves (15-point averaging interval). Designations: 1st half, 1st half of the ranked mouse cohort; 2nd half, 2nd half of the ranked mouse cohort; odd, odd individuals of the mouse ranked cohort; even, even individuals of the mouse ranked cohort; solid vertical lines, major peak midlines; dashed lines, cluster borders.

tually no dependence on the procedure used to separate mice into subgroups.

The absence of significant differences between the positions of the corresponding clusters on the lifespan axis (Figs. 2 and 4, Tables 1 and 2) suggest age-related programming of increased death rate in mouse ontogenesis. Therefore, my earlier conclusion [5-8] on the insufficiency of the two-parameter Gompertz model [1] and its tri-parameter modification suggested by Makeham [2, 9] for describing mouse mortality has been experimentally demonstrated.

The discovery of reproducible peaks and clusters of increased mortality in mouse ontogenesis is in close agreement with the concept of programmed death of an entire organism, the so-called phenoptosis concept developed by V. P. Skulachev [10]. Since the periods of increased mortality risk in mouse ontogenesis resemble

the periods of defoliation in plants, mouse phenoptosis appears to be similar to plant apoptosis. It is possible to suggest that in evergreens, in which defoliation occurs independently of the season-related weather changes, the lifespans of individual leaves (as measured from the germ formation in the leaf buds or bud opening) have the same step-wise character as the lifespans of mice reflected in their mortality curves.

Identification of programmed peaks and clusters of peaks of increased mortality in mouse ontogenesis is only the early phenomenological level of investigation. What are the prospects of further study of such peaks and peak clusters and their practical application? Apparently, a similar phenomenon has not yet been shown to exist in humans.

Even if positions of peaks and their clusters on the lifespan axis are sufficiently stable characteristics, the heights of these peaks and the clusters vary significantly. This might be explained by their sensitivity to external factors. Searching for new methods of identification of programmed mortality risks and efficient regulation of the organism's state during the period of ontogenesis that correspond to the increased mortality peaks might be a very promising direction in medicine. Because in mice the mortality rate at the tops of the peaks in most cases significantly exceeds the mortality rate at the bases of the peaks (as demonstrated in [5]), lowering the peak heights to the basal level opens new prospects for solving the

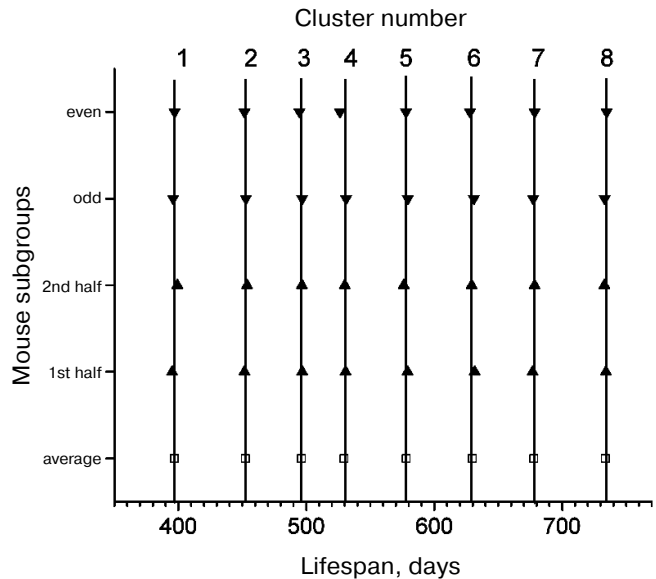


Fig. 4. Weighed positions of eight clusters on lifespan curves obtained by rolling averaging of initial mortality curves (15-point averaging interval) relative to the mean arithmetic positions of the clusters. Designations: 1st half, 1st half of the ranked mouse cohort; 2nd half, 2nd half of the ranked mouse cohort; odd, odd individuals of the ranked mouse cohort; even, even individuals of the ranked mouse cohort; average, mean arithmetic positions of the clusters (designated by vertical lines).

problem of early death in humans. One of the promising means that could be used for this purpose is compounds of the SkQ developed by V. P. Skulachev and his colleagues [10, 11].

Except in cases of sudden death, death of an organism is usually preceded by diseases with symptoms that can be used to diagnose and to prescribe certain treatment. There are some known cases of self-healing in the absence of any medical intervention that indicate that treatment resulting in the percentage of lethal outcomes comparable to that in nontreated individuals is inefficient. In these cases, we suggest that recovery depends on the stage of ontogenesis at which some external factor provoked the disease, i.e., was it at the beginning of the increased mortality risk period or at its end? Therefore, lethal outcome might be determined not by the disease itself, but rather by simultaneous effect of several factors, e.g., combination of infection and entrance of an organism into a genetically programmed critical period of development.

Perhaps the identified clusters correspond to a programmed predisposition to chronic disorders (diabetes, cancer, osteoporosis, etc.) accompanied by increased mortality risk. The peaks that comprise the clusters presumably correspond to disease exacerbations leading to death, with probability that is proportional to the peak size. If this is true, then the intervals between the peaks in the clusters could be considered as periods of remission.

The absence of a corresponding peak on one of the compared differential curves in the independent mouse subgroups would suggest that all mice of this age in the subgroup experience conditions that allow them to overcome the risk of death and transit to the next stable developmental stage. This situation resembles self-healing in medical practice. Therefore, intensive prophylactics of diseases should precede the ages of increased mortality risk and continue until the next periods of stable development.

We can assume that the identified peaks of mortality are typical only for the normal mice from the offspring obtained by crossing mutant males with normal females, as done in this study. To confirm this assumption, the same type of experiments should be performed in mice resistant to changes in the progeny or in other animal species. However, the existence of reproducible step-wise changes at the same ages in the mortality and survivorship curves observed in other studies favors the suggestion that death programming in ontogenesis is a universal phenomenon. As an example, note the similarities in the positions of inflexions in the survivorship graphs for different mouse groups in the two-volume textbook by Anisimov [12], which unfortunately had been left outside of the scope of author's attention.

Even more important is the high degree of coincidence between the weighed mean positions of mortality clusters on the lifespan axis (Tables 1 and 2, Figs. 2 and

4), which can be formally interpreted as a manifestation of some curve that has a maximum and describes random distribution of the peaks by their height. However, this seemingly random event might mask some hidden regularities that require further investigations. The observed higher reproducibility of the position of the maximum of this hypothetical curve compared to the major peaks representing clusters in the first approximation might be explained by compensation of the major peak shifts by the surrounding minor peaks. The latter becomes more understandable if we assume that clusterization results not from merging of several peaks, but rather from splitting of one big peak, e.g., due to disturbances in the genetic homogeneity of the studied mouse population. However, possible mechanisms for each of these alternative processes remain obscure.

In conclusion, it is pertinent to note that the combination of individual elements of natural systems into clusters is a universal phenomenon. As examples, I mention spectral lines in the optical spectra of molecules that can be observed at sufficient resolution, or stars that form clusters and nebulae in astronomy. Even chemical elements of the periodic system could be viewed as clusters of isotopes. Thus, experimentally obtained atomic weights of elements coincide with those calculated from the atomic masses of isotopes and the data on the isotope relative content in natural objects by a formula that is similar to formula (6). Therefore, the presence of clusters composed of mortality peaks in mouse ontogenesis should be considered another manifestation of the tendency for clusterization of elementary phenomena in nature. Proving the existence of reproducible mortality peaks and peak clusters in human ontogenesis would make it possible to direct gerontology from fruitless searches for the universal elixir of youth to more promising studies of genetically programmed death risks and methods for their prevention.

Acknowledgments

The author thanks L. A. Denisova (Animal Facility, Bach Institute of Biochemistry, Russian Academy of Sciences) for help with the experiment and E. S. Pshennikova for proofreading of the manuscript.

REFERENCES

1. Gompertz, B. (1825) On the nature of the function expressive of the law of human mortality and on a new mode of determining the value of life contingencies, *Philos. Trans. Roy. Soc. London A*, **115**, 513-583.
2. Gavrilov, L. A., and Gavrilova, N. S. (1991) *Biology of Longevity* [in Russian], Nauka, Moscow.
3. Lamb, M. J. (1977) *Biology of Aging*, Blackie, Glasgow.

4. Mylnikov, S. V., Oparina, T. I., and Bychkovskaya, I. B. (2015) On the discontinuous character of annuity curves. Communication I. Deviations from the Gompertz law in *Drosophila melanogaster* Canton-S line, *Usp. Gerontol.*, **28**, 624-628.
5. Malygin, A. G. (2017) New data on programmed risks of death in normal mice and mutants with growth delay, *Biochemistry (Moscow)*, **82**, 834-843.
6. Malygin, A. G. (2012) Variations in the lifespan of mice during the periods of growth and aging, *Dokl. MOIP Sect. Gerontol.*, **50**, 56-65.
7. Malygin, A. G. (2013) Graduated change of life expectancy in mice ontogenesis, *Rus. J. Dev. Biol.*, **44**, 48-55.
8. Malygin, A. G. (2013) Age fluctuations in mortality of mice with mutation causing growth retardation, *Biochemistry (Moscow)*, **78**, 1033-1042.
9. Makeham, W. M. (1860) On the law of mortality and the construction of annuity tables, *J. Inst. Actuaries*, **8**, 301-310.
10. Skulachev, V. P. (2012) What is "phenoptosis" and how to fight it? *Biochemistry (Moscow)*, **77**, 827-846.
11. Skulachev, V. P., Skulachev, M. V., and Fenyuk, B. A. (2014) *Life without Aging* [in Russian], EKSMO, Moscow.
12. Anisimov, V. N. (2008) *Molecular and Physiological Mechanisms of Aging* [in Russian], Nauka, St. Petersburg.